広島大学学術情報リポジトリ
Hiroshima University Institutional Repository

Title	Synthesis of high-silica CHA type zeolite by interzeolite conversion of FAU type zeolite in the presence of seed crystals
Auther(s)	Itakura, Masaya; Goto, Ikuhiro; Takahashi, Atsushi; Fujitani, Tadahiro; Ide, Yusuke; Sadakane, Masahiro; Sano, Tsuneji
Citation	Microporous and Mesoporous Materials , 144 (1-3) : 91 - 96
Issue Date	2011
DOI	10.1016/j.micromeso.2011.03.041
Self DOI	
URL	http://ir.lib.hiroshima-u.ac.jp/00034805
Right	(c) 2011 Elsevier B.V. All rights reserved.
Relation	

Hiroshima University Institutional Repository

(Revised)

Synthesis of high-silica CHA type zeolite by interzeolite conversion of FAU type zeolite in the presence of seed crystals

Masaya Itakura[a], Ikuhiro Goto[a], Atsushi Takahashi[b], Tadahiro Fujitani[b], Yusuke Ide[a], Masahiro Sadakane[a], Tsuneji Sano[a],*

[a] Department of Applied Chemistry, Graduate School of Engineering, Hiroshima University, Higashi-Hiroshima 739-8527, Japan

[b] Research Institute for Innovation in Sustainable Chemistry, National Institute of Advanced Industrial Science and Technology, Tsukuba, Ibaraki 305-8569, Japan

*Corresponding author: Fax: +81-82-424-5494; Phone: +81-82-424-7607; E-mail:

tsano@hiroshima-u.ac.jp

Abstract

    The influence of seed crystals on the interzeolite conversion of FAU type zeolite into CHA type zeolite was investigated in the presence of benzyltrimethylammonium hydroxide as a structure-directing agent under various hydrothermal synthesis conditions. Pure and highly

crystalline CHA type zeolites with a wide range of Si/Al ratios were obtained in a shorter

crystallization time as compared with those obtained without seed crystals. Furthermore, we

achieved the first successful synthesis of high-silica CHA type zeolite in the absence of Na^+ cations

by increasing the seed content. The protonated CHA type zeolite with a Si/Al ratio of ca. 15 yielded

the highest propylene yield of ca. 48 C-% in ethanol conversion into light olefins.

1. Introduction

   Aluminosilicate zeolite chabazite (CHA) with Si/Al ratios of 2–3 has a three-dimensional pore

system with ellipsoidal-shaped large cages (6.7 × 10 Å) that are accessible via 8-membered ring

windows (3.8 × 3.8 Å). High-silica chabazite SSZ-13 and silicoaluminophosphate zeotype SAPO-34

characterized by CHA structure have attracted great interest because they exhibit specific shape

selectivity for the conversion of methanol [1–3] or bioethanol [4,5] into light olefins such as ethylene

and propylene. Pure silica chabazite also has potential applications involving adsorption and

separation of organic molecules and gas storage on account of a larger void space attributable to the

absence of counter cations in the pores and to its extreme hydrophobicity. SSZ-13 and pure silica

chabazite have been synthesized only in alkali or fluoride media using expensive N,N,N-trimethyl-adamantammonium cation (TMAda$^+$) as a structure-directing agent (SDA) [6,7].

Recently, we investigated the potential for interzeolite conversion — hydrothermal conversion of one zeolite into another — which has attracted much attention as an alternative strategy for zeolite synthesis. We have succeeded in synthesizing several types of zeolites, such as *BEA, LEV, MTN, OFF, and RUT, from FAU type zeolite in the presence of a variety of SDAs [8–12]. The crystallization rate of zeolite with FAU type zeolite was greater than that with aluminosilicate gel (the conventional synthesis). The enhancement in the crystallization rate occurs because the decomposition/dissolution of the starting zeolite generates locally ordered aluminosilicate species (nanoparts) that assemble and evolve into another type of zeolite.

Very recently, we also succeeded in synthesizing high-silica CHA type zeolite from FAU type zeolite using benzyltrimethylammonium cation (BTMA$^+$) instead of a typical SDA, namely, the expensive TMAda$^+$ cation [13]. The protonated CHA type zeolite exhibited good catalytic performance for conversion of ethanol to light olefins, with product yields of 54.7 C-% ethylene and 35.1 C-% propylene. However, a prolonged crystallization time (up to 21 days) was required, and the Si/Al ratio range (16–17) of the obtained CHA type zeolite was surprisingly narrow.

In general, it is well known that adding seed crystals of the desired zeolite phase to the starting synthesis gel can enhance the crystallization rate [14–17]. Moreover, it is also possible to control the

crystal size distribution in this manner [18,19]. Although the mechanism of the crystallization rate

enhancement has not been clarified, two explanations have been offered [20]: (1) the increase in the

surface area due to the addition of the seed crystals results in an increased and faster consumption of

reagents and (2) seeds promote nucleation through some secondary nucleation mechanism.

From such viewpoints, in this study we attempted the facile synthesis of high-silica CHA type

zeolite by interzeolite conversion of FAU type zeolite in the presence of seed crystals. Moreover, the

catalytic performance of the obtained high-silica CHA type zeolite was investigated based on ethanol

conversion reactions.

2. Experimental

2.1. Synthesis of CHA type zeolite

The starting FAU type zeolites with various Si/Al ratios were prepared from NH_4-Y zeolite (Si/Al

= 2.8, Tosoh Co., Japan) by carrying out dealumination treatment involving a combination of

steaming at 700 °C and H_2SO_4 (0.74–0.85 M) treatment at 75 °C for 4 h. **Seed crystals (CHA type**

zeolite, Si/Al = 16) were synthesized according to the method used in our previous study [13],

and protonated using a 1 M of NH_4NO_3 solution, followed by calcination at 450 °C for 10 h,

giving Na$^+$ cation-free seed crystals. The hydrothermal conversion was performed as follows: The dealuminated FAU type zeolite was thoroughly mixed with an aqueous solution containing BTMAOH (40 wt%, Aldrich, USA) as an SDA, seed crystals, and, optionally, an additive (NaOH (>99%, High Purity Chemical Inc., Japan) or NaCl (>99.5%, Kanto Chemical Co. Inc., Japan)). Then, the mixture was placed into a 30 cm^3 Teflon-lined stainless steel autoclave. The hydrothermal conversion was conducted at 125 °C for 7–21 days in the convection oven. After crystallization, the reaction mixture was cooled to room temperature, and the solid phase was separated from the liquid phase by centrifugation. The solid product was washed thoroughly with deionized water until a near neutral pH was achieved, and it was dried overnight at 70 °C and calcined at 600 °C for 10 h to remove SDA cations occluded in the zeolite pores. The detailed hydrothermal conversion conditions are listed in Table 1.

2.2. Characterization

Powder X-ray diffraction (XRD) patterns of the solid products were collected on a Rigaku Mini Flex diffractometer with curved-graphite monochromatized Cu-Kα radiation operated at 30 kV and 15 mA. Si/Al ratios of the calcined samples were analyzed using the dilithium tetraborate (Li$_2$B$_4$O$_7$) method with the X-ray fluorescence (XRF) technique (Philips PW 2400). In these experiments, 0.5 g

of sample was fused with 5 g of $Li_2B_4O_7$ at 1100 °C. The Si/Al ratio was calculated from the Si and

Al concentrations, which were determined by the corresponding calibration curves that were

prepared using high purity SiO_2 (99.999%) and γ-Al_2O_3 (99.999%). The crystal morphology was

observed using scanning electron microscopy (SEM, HITACHI S-5200). Nitrogen adsorption

isotherms at −196 °C were obtained using a conventional volumetric apparatus (Bel Japan,

BELSORP 28SA). ^{27}Al and ^{29}Si MAS NMR spectra were recorded using a 7 mm–diameter zirconia

rotor on a Bruker Avance DRX-400 operating at 104.3 MHz and 79.5 MHz, respectively. The rotor

was spun at 9 kHz for ^{27}Al MAS NMR and 4 kHz for ^{29}Si MAS NMR. The spectra were

accumulated with 2.3 μs pulses, 1 s and 1000 scans for ^{27}Al MAS NMR and 5 μs, 20 s and 2000

scans for ^{29}Si MAS NMR. $Al(NO_3)_3 \cdot 9H_2O$ and $Si(CH_3)_4$ were used as chemical shift references for

^{27}Al MAS NMR and ^{29}Si MAS NMR, respectively. Prior to the ^{27}Al MAS NMR measurement, the

sample was moisture equilibrated over a saturated solution of NH_4Cl for 24 h. Thermal analyses

were carried out using a TG/DTA apparatus (SSC/5200 Seiko Instruments). A sample (ca. 7 mg) was

heated in a flow of air (50 mL min^{-1}) at a heating rate of 5 °C min^{-1} from room temperature to

800 °C.

2.3. Catalytic testing

The catalytic performance of the protonated CHA type zeolite (H-CHA) for the ethanol

conversion reaction was tested using a quartz fixed-bed reactor at 400 °C and atmospheric

pressure. The protonated form was prepared using an ion-exchange method with a 1 M NH_4NO_3

solution, followed by calcination at 450 °C for 10 h. The reaction gas, $EtOH/N_2$ (50/50 vol%),

was fed at a W/F (g (H-CHA)/mL ($EtOH/N_2$) per min) of 0.0125–0.03 g min mL^{-1}. **The gaseous**

products were analyzed through on-time GC equipped with TCD- and FID-type detectors,

on Shincarbon ST (Shinwa Chem. Ind. Ltd., Japan) for N_2, H_2, and CO_2; on Gaskropack54 (GL

Sciences, Japan) for ethanol; and on RT-alumina PLOT (Restek, USA) for C_1–C_4 hydrocarbons.

The product yields were calculated using N_2 as an internal standard.

3. Results and Discussion

3.1. Synthesis and characterization of high-silica CHA type zeolite

When the hydrothermal conversion of FAU type zeolite was carried out in the absence of seed

crystals, a prolonged crystallization time (21 days) was required for synthesis of highly crystalline

CHA type zeolite (sample no. 1 in Table 1). The FAU–CHA interzeolite conversion did not occur

when the Si/Al ratio of the starting FAU type zeolite was 25 (sample no. 2). When the 2 wt% seed

crystals were added to the starting gel, however, highly crystalline CHA type zeolite was obtained

after hydrothermal treatment for only 7 days (sample no. 5). The yield of CHA type zeolite was ca.

92% based on the weight of the FAU type zeolite. Fig. 1 provides the XRD patterns of the CHA type

zeolites obtained in the absence and in the presence of seed crystals. They show the typical

diffraction pattern of a CHA type zeolite, which contains no impurities from unconverted starting

FAU type zeolite or from a co-crystallized phase. There was no difference in the peak intensity of the

two CHA type zeolites. For comparison, we attempted to synthesize CHA type zeolite from

amorphous $SiO_2/\gamma\text{-}Al_2O_3$ as the starting material (sample no. 16). However, CHA type zeolite was

not obtained, demonstrating the advantage and uniqueness of the hydrothermal conversion of FAU

type zeolite.

Our previous results concerning the interzeolite conversion showed that the conversion was

strongly dependent on the Si/Al ratio of the starting FAU type zeolite [8–13]. In order to study the

influence of the Si/Al ratio of the starting FAU type zeolite on the synthesis of CHA type zeolite,

FAU type zeolites with various Si/Al ratios (Si/Al = 16–95) were prepared through dealumination

treatment and were subjected to hydrothermal treatment. For the FAU type zeolites with Si/Al ratios

of 16 and 30, a prolonged synthesis time (14 days) was needed (sample nos. 4 and 6). However, for

the Si/Al ratio of 44, pure CHA type zeolite was not obtained (sample no. 7). When NaOH was used

as an additive instead of NaCl, pure CHA type zeolites were obtained from starting FAU type

zeolites with higher Si/Al ratios (sample nos. 10 and 11). However, the Si/Al ratios of the obtained

CHA type zeolites were considerably smaller than those of the starting FAU type zeolites. The lower

Si/Al ratio is probably due to the higher alkalinity of the hydrothermal conversion, namely, an

increase of silicon concentration in the liquid phase.

Fig. 2 presents SEM images of CHA type zeolites obtained from FAU type zeolite, together with

the starting FAU type zeolite. After thorough observation, we did not find any crystals of the starting

FAU type zeolite or impurities. In the SEM image of the CHA type zeolite obtained without seed

crystals, ellipsoidal plate-like crystals with a size of 1–1.5 μm were observed (Fig. 2 (b)). On the

other hand, CHA type zeolite obtained with seed crystals exhibited a cubic morphology, and the

crystal size was 100–200 nm (Fig. 2 (c)).

Next, to clarify the chemical states of aluminum and silicon in the obtained CHA type zeolite, ^{27}Al

and ^{29}Si MAS NMR measurements were performed. Fig. 3 provides the ^{27}Al MAS NMR spectra of

CHA type zeolites obtained without and with seed crystals. Regardless of the presence of seed

crystals, only one peak centered at ca. 55 ppm was observed, corresponding to tetrahedrally

coordinated aluminum species. The peak corresponding to octahedrally coordinated aluminum

species, i.e., extra-framework aluminum species, was not observed at around 0 ppm. This means that

all of the aluminum species present in both CHA type zeolites resulting from hydrothermal

conversion of FAU type zeolite exist within the zeolite framework. The ^{29}Si MAS NMR spectra of

9

these CHA type zeolites are also shown in Fig. 4. Three peaks were observed centered at ca. −110,

−105, and −100 ppm, and they are assigned to Q^4(0Al), Q^4(1Al), and Q^4(2Al) + Q^3(0Al),

respectively (Fig. 4) [21,22]. The difference in the intensity of the peak at ca. −105 ppm of the CHA

type zeolites is due to the difference in the aluminum content. The BET surface area and the

micropore volume of the CHA type zeolite obtained with seed crystals were calculated to be 630

m^2g^{-1} and 0.29 m^2g^{-1}, respectively, and those calculated from the CHA type zeolite obtained without

seed crystals were 590 m^2g^{-1} and 0.29 m^2g^{-1}.

In our previous studies, alkaline metal cations, especially Na^+ cations, were required for synthesis

of LEV, MTN, and OFF type zeolites from FAU type zeolite [9–11]. To clarify the role of Na^+

cations in the FAU–CHA interzeolite conversion process, the interzeolite conversion was carried out

in the absence of NaCl. Although a higher $BTMAOH/SiO_2$ ratio and seed content were needed, the

FAU–CHA interzeolite conversion proceeded effectively (sample nos. 13–15 in Table 1). It was

thereby found that Na^+ cations are not required for interzeolite conversion in the presence of seed

crystals. To our knowledge, this is the first report on alkaline metal cation–free synthesis of

high-silica CHA type zeolite. As can be seen in Fig. 2 (d), the crystal size of Na^+ cation–free CHA

type zeolite was considerably smaller than that obtained in the presence of Na^+ cations, suggesting

an enhancement of nucleation. Fig. 5 presents FT-IR spectra in the hydroxyl groups region of the

protonated CHA type zeolites (H-CHA) obtained in the absence and in the presence of Na^+ cations.

The CHA type zeolite obtained in the presence of Na^+ cations was protonated by ion-exchange with

a 1 M NH_4NO_3 solution, followed by calcination at 450 °C for 10 h. On the other hand, the Na^+

cation–free CHA type zeolite was protonated only by calcination. The IR spectrum of the H-CHA

type zeolite obtained in the presence of Na^+ cations exhibited four peaks at approximately 3730,

3680, 3610, and 3500 cm^{-1}. The two peaks at 3730 and 3610 cm^{-1} are assigned to isolated silanol

groups and to the acidic bridged OH of Si(OH)Al, respectively, whereas the peaks at 3680 and 3500

cm^{-1} are assigned to internal silanol groups of hydroxyl nests [23]. The intensity of the peak at 3500

cm^{-1} was slightly strong in the spectrum of the H-CHA type zeolite obtained in the absence of Na^+

cations. These results indicate that the H-CHA type zeolite in the absence of Na^+ cations is higher in

framework defects.

3.2. Ethanol to olefins reaction

Regarding the high-silica CHA type zeolites with a wide range of Si/Al ratios that were obtained

by interzeolite conversion of FAU type zeolite in the presence of seed crystals, their catalytic

performance for ethanol conversion to light olefins was evaluated using a fixed-bed reactor at

atmospheric pressure and a temperature of 400 °C, with W/F = 0.0125 g min mL^{-1}. The typical

results over CHA type zeolites obtained with and without seed crystals are shown in Fig. 6. For both

H-CHA type zeolites, the ethanol conversion was 100%, even after 3 h time on stream. The initial

propylene yield for CHA type zeolite obtained with seed crystals (sample no. 5) was ca. 10 C-%

higher than that for CHA type zeolite obtained without seed crystals (sample no. 1). **The yields of**

products obtained on the CHA type zeolite synthesized with seed crystals were as follows: 37.1

C-% ethylene, 45.4 C-% propylene, 3.0 C-% butene, 6.0 C-% C_1–C_5 paraffins and 7.4 C-%

C_5^+ species. However, rapid deactivation by the poisoning of acid sites due to the accumulation

of carbonaceous deposits was observed. The amounts of carbonaceous deposits after a reaction

lasting 3 h, evaluated by TG analysis, were 19.8% and 16.9% for CHA type zeolites obtained with

and without seed crystals, respectively.

Fig. 7 shows the relationship between the Si/Al ratio of CHA type zeolite obtained with seed

crystals and initial ethylene and propylene yields at 0.5 h time on stream. The ethylene and

propylene yields were strongly dependent on the Si/Al ratio, and the maximum propylene yield of ca.

48 C-% was obtained at the Si/Al ratio of ca. 15. On the other hand, the ethylene yield tended to

increase with an increase in the Si/Al ratio. **As it is well known that the product distribution in**

the zeolitic ethanol conversion process strongly depends on the acidity as well as the channel

structure of zeolite and that ethanol is considered to first convert to ethylene and then

subsequently to higher hydrocarbons, the observed relationship between the Si/Al ratio and

initial ethylene and propylene yields seems to be related with the oligomerization ability of

ethylene on the acid sites. Next, therefore, the effect of ethylene consumption on the propylene

yield was investigated [24]. The propylene yield was plotted against the ethylene consumption rate

(%, 100 – yield of ethylene), as shown in Fig. 8. To obtain a variety of ethylene consumption values,

the ethanol conversion reaction was carried out at 400 °C while varying the W/F ratio. The

propylene yield increased with an increase in the ethylene consumption rate, and it reached a

maximum yield of ca. 48 C-% at ca. 72% ethylene consumption rate. This value is similar to that of

SAPO-34 (52.2 C-% at 71.2% ethylene consumption) having a CHA type structure **[4].**

4. Conclusions

In this study, we reported FAU–CHA interzeolite conversion in the presence of seed crystals. By

adding seed crystals together with Na$^+$ cations, CHA type zeolites with a wide range of Si/Al ratios

(13.4–21.5) were obtained with shorter crystallization time (7–14 days). The addition of seed

crystals reduced the crystal size from ca. 1.5 μm to 200 nm. We also achieved the first successful

synthesis of high-silica CHA type zeolite in the absence of Na$^+$ cations by using a higher content of

seed crystals, indicating that no H$^+$ ion-exchange process is required for the use of a solid acid

catalyst. The protonated CHA type zeolite exhibited good performance in relation to the conversion

of ethanol to light olefins. A maximum propylene yield of ca. 48 C-% was achieved at the Si/Al ratio

of ca. 15.

References

[1] M. Stöcker, Micropor. Mesopor. Mater. 29 (1999) 3.

[2] J.Q. Chen, A. Bozzano, B. Glover, T. Fuglerud, S. Kvisle, Catal. Today 106 (2005) 103.

[3] Q. Zhu, J.N. Kondo, T. Tatsumi, S. Inagaki, R. Ohnuma, Y. Kubota, Y. Shimodaira, H. Kobayashi,

K. Domen, J. Phys. Chem. C 111 (2007) 5409.

[4] H. Oikawa, Y. Shibata, K. Inazu, Y. Iwase, K. Murai, S. Hyodo, G. Kobayashi, T. Baba, Appl.

Catal. A 312 (2006) 181.

[5] M. Yamaguchi, Y. Yoshikawa, T. Takewaki, R. Setoyama, Jpn. Kokai Tokkyo Koho 2007-291076

(2007).

[6] M.J. Díaz-Cabañas, P.A. Barrett, M.A. Camblor, Chem. Commun. 17 (1998) 1881.

[7] S.I. Zones, US Patent 4,544,538 (1985).

[8] H. Jon, K. Nakahata, B. Lu, Y. Oumi, T. Sano, Micropor. Mesopor. Mater. 96 (2006) 72.

[9] T. Inoue, M. Itakura, H. Jon, Y. Oumi, A. Takahashi, T. Fujitani, T. Sano, Micropor. Mesopor.

Mater. 122 (2009) 149.

[10] H. Sasaki, H. Jon, M. Itakura, T. Inoue, T. Ikeda, Y. Oumi, T. Sano, J. Porous Mater. 16 (2009)

465.

[11] M. Itakura, Y. Oumi, M. Sadakane, T. Sano, Mater. Res. Bull. 45 (2010) 646.

[12] H. Jon, S. Takahashi, H. Sasaki, Y. Oumi, T. Sano, Micropor. Mesopor. Mater. 113 (2008) 56.

[13] M. Itakura, T. Inoue, A. Takahashi, T. Fujitani, Y. Oumi, T. Sano, Chem. Lett. 39 (2008) 908.

[14] G.T. Kerr, J. Phys. Chem. 70 (1966) 1047.

[15] G.T. Kerr, J. Phys. Chem. 72 (1968) 1385.

[16] J. Warzywoda, R.W. Thompson, Zeolites 11 (1991) 577.

[17] B. Lu, T. Tsuda, Y. Oumi, K. Itabashi, T. Sano, Micropor. Mesopor. Mater. 76 (2004) 1.

[18] C.S. Cundy, P.A. Cox, Micropor. Mesopor. Mater. 82 (2005) 1.

[19] C.S. Cundy, J.O. Forrest, in: A. Galarneau, F. Di Renzo, F. Fajula, J. Vedrine (Eds.), Proc.

13th Int. Zeolite Conf., Stud. Surf. Sci. Catal. 135 (2001) 185.

[20] K. Nishi, R.W. Thompson, in: K Schüth, S.W. Sing, J. Weitkamp (eds.), Handbook of Porous

Solids, vol. 2, WILEY-VCH, Germany, 2002, 736.

[21] D.E. Akporiaye, I.M. Dahl, H.B. Mostad, R. Wendelbo, J. Phys. Chem. 100 (1996) 4148.

[22] M.A. Camblor, A. Corma, M.-J. Díaz-Cabaňas, J. Phys. Chem. B 102 (1998) 44.

[23] G.L. Wooley, L.B. Alernany, R.M. Dessau, A.W. Chester, Zeolites 6 (1986) 14.

[24] Y. Iwase, K. Motokura, T. Koyama, A. Miyaji, T. Baba, Phys. Chem. Chem. Phys. 11 (2009)

9268.

Table 1 Hydrothermal conversion of FAU type zeolite and products obtained.

| Sample no. | Synthesis conditions[a] | | | | | Product | | | |
	Starting Si/Al ratio	BTMAOH/SiO$_2$ ratio	Additive	Seed content /wt%	Time /days	Phase[b]	Bulk Si/Al ratio	S_{BET} /m^{2}g^{-1}	Micropore volume /cm^{3}g^{-1}
1	22	0.2	NaCl		21	CHA	16.9	590	0.29
2	25	0.2	NaCl		21	Am.			
3	16	0.2	NaCl	2	7	FAU,CHA,Am.			
4	16	0.2	NaCl	2	14	CHA	14.5		
5	22	0.2	NaCl	2	7	CHA	18.2	630	0.29
6	30	0.2	NaCl	2	14	CHA	21.5		
7	44	0.2	NaCl	2	14	CHA,Am.			
8	16	0.2	NaOH	2	7	CHA	14.7		
9	22	0.2	NaOH	2	7	CHA	14.7	590	0.30
10	81	0.2	NaOH	2	7	CHA	21.3		
11	95	0.2	NaOH	2	7	CHA	19.6		
12	24	0.3		2	14	Am.,CHA			
13	24	0.3		5	14	CHA	14.0		
14	22	0.3		10	7	CHA	13.6	620	0.29
15	97	0.3		10	7	CHA	18.6		
16[c]	22	0.2	NaCl	2	14	Lay.,Am.			

[a] H$_2$O/SiO$_2$ = 5, Additive/SiO$_2$ = 0.1, Temp. = 125 °C

[b] Am. = amorphous, Lay. = layered material

[c] Amorphous silica and γ-Al$_2$O$_3$ were used as starting materials.
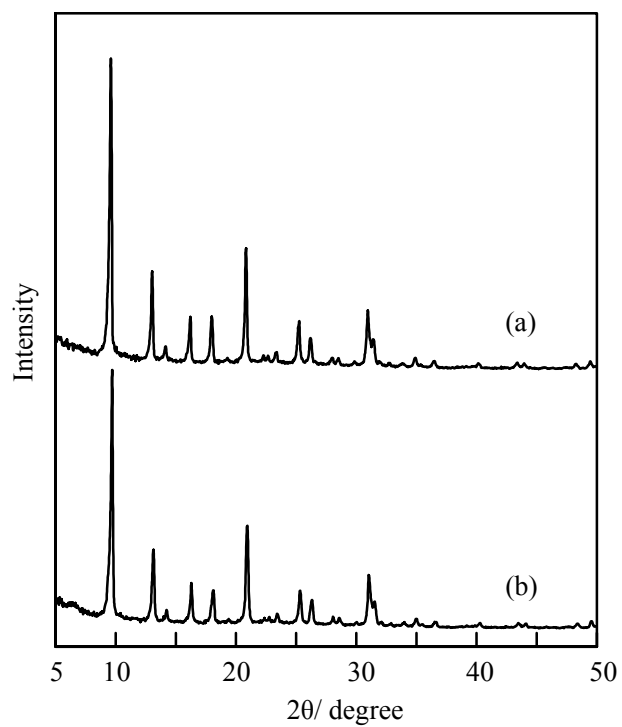
Figure captions

Fig. 1 XRD patterns of CHA type zeolites obtained (a) without seed crystals (sample no. 1) and (b)
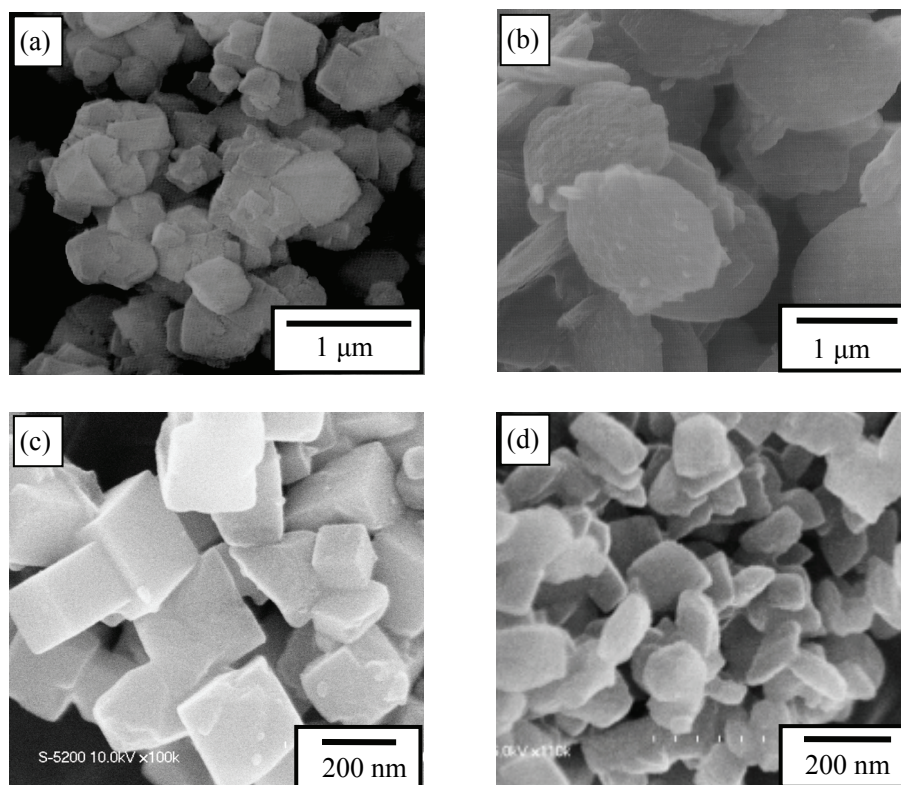
with seed crystals (sample no. 5).

Fig. 2 SEM images of starting FAU type zeolite and various CHA type zeolites obtained. (a) FAU

type zeolite, (b) CHA type zeolite obtained without seed crystals (sample no. 1), (c) CHA type

zeolite obtained with seed crystals (sample no. 5), and (d) CHA type zeolite obtained with seed

crystals in the absence of Na^+ cations (sample no. 15).

Fig. 3 ^{27}Al MAS NMR spectra of CHA type zeolites obtained (a) without seed crystals (sample no.

1) and (b) with seed crystals (sample no. 5).

Fig. 4 ^{29}Si MAS NMR spectra of CHA type zeolites obtained (a) without seed crystals (sample no. 1)

and (b) with seed crystals (sample no. 5).

Fig. 5 FT-IR spectra of H-CHA type zeolites. (a) CHA type zeolite obtained with seed crystals in the

presence of NaCl (sample no. 5) and (b) Na^+ cation−free CHA type zeolite obtained with seed

crystals (sample no. 15).

Fig. 6 Time on stream of propylene yield and ethanol conversion of CHA type zeolites obtained with seed crystals (■, ▲), sample no. 5, and without seed crystals (□, △), sample no. 1. Reaction conditions: temp. = 400 °C, W/F = 0.0125 g min mL^{-1}.

Fig. 7 Relationship between Si/Al ratio of CHA type zeolite and yield of light olefins ((□) ethylene and (■) propylene). Reaction conditions: temp. = 400 °C, W/F = 0.0125 g min mL^{-1}.

Fig. 8 Propylene yield as a function of ethylene consumption rate for CHA type zeolite obtained with seed crystals.

Fig. 1 XRD patterns of CHA type zeolites obtained (a) without seed crystals (sample no. 1) and (b) with seed crystals (sample no. 5).

Fig. 2 SEM images of starting FAU type zeolite and various CHA type zeolites obtained. (a) FAU type zeolite, (b) CHA type zeolite obtained without seed crystals (sample no. 1), (c) CHA type zeolite obtained with seed crystals (sample no. 5), and (d) CHA type zeolite obtained with seed crystals in the absence of Na^+ cations (sample no. 15).
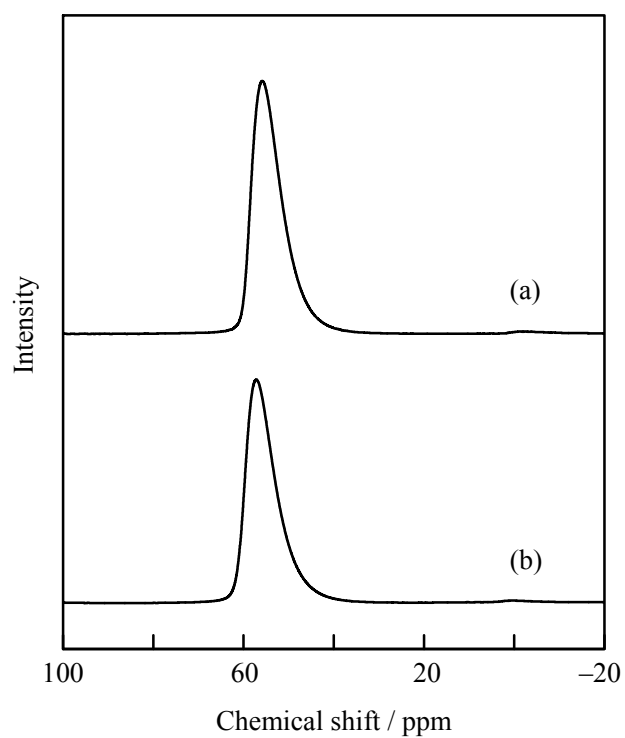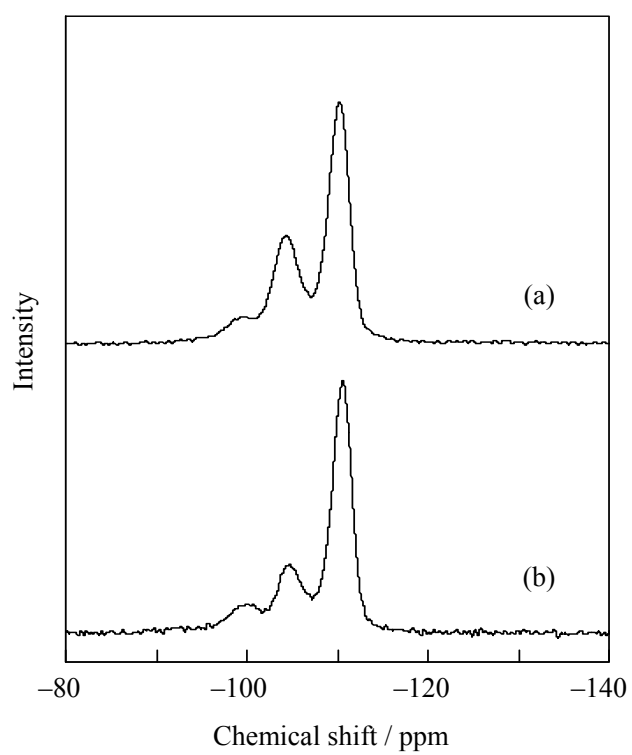
Fig. 3 ^{27}Al MAS NMR spectra of CHA type zeolites
obtained (a) without seed crystals (sample no. 1) and
(b) with seed crystals (sample no. 5).

Fig. 4 ^{29}Si MAS NMR spectra of CHA type zeolites obtained (a) without seed crystals (sample no. 1) and (b) with seed crystals (sample no. 5).
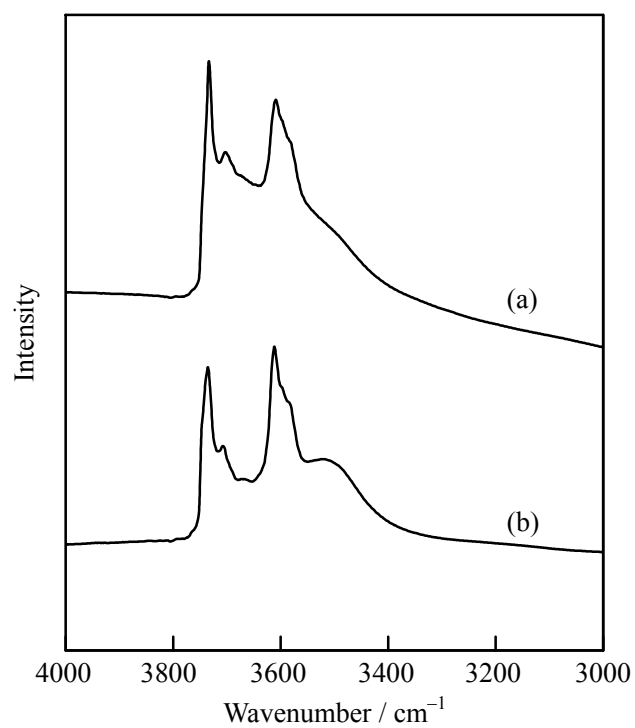
Fig. 5 FT-IR spectra of H-CHA type zeolites. (a) CHA type zeolite obtained with seed crystals in the presence of NaCl (sample no. 5) and (b) Na$^+$ cation–free CHA type zeolite obtained with seed crystals (sample no. 15).
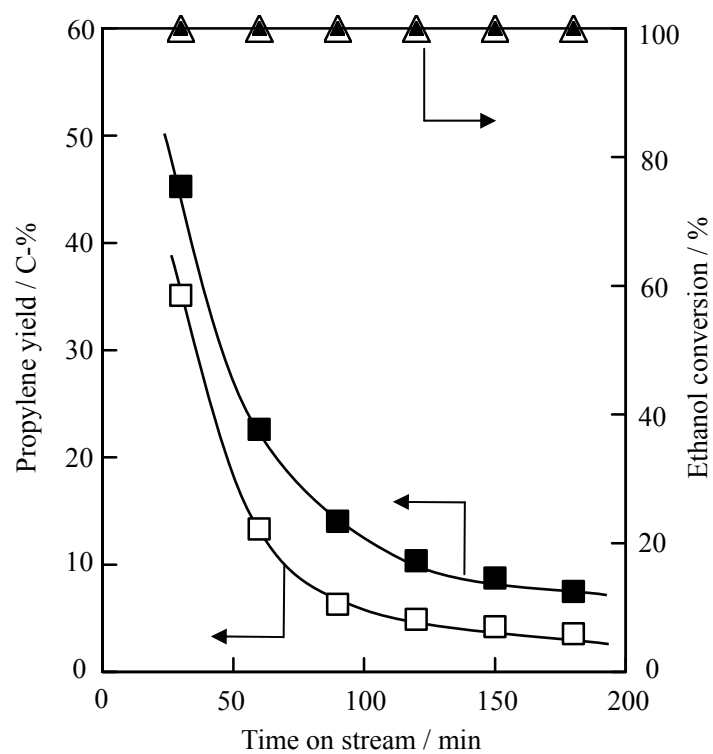
Fig. 6 Time on stream of propylene yield and ethanol conversion of CHA type zeolites obtained with seed crystals (■, ▲), sample no. 5, and without seed crystals (□, △), sample no. 1. Reaction conditions: temp. = 400 °C, W/F = 0.0125 g min mL^{-1}.
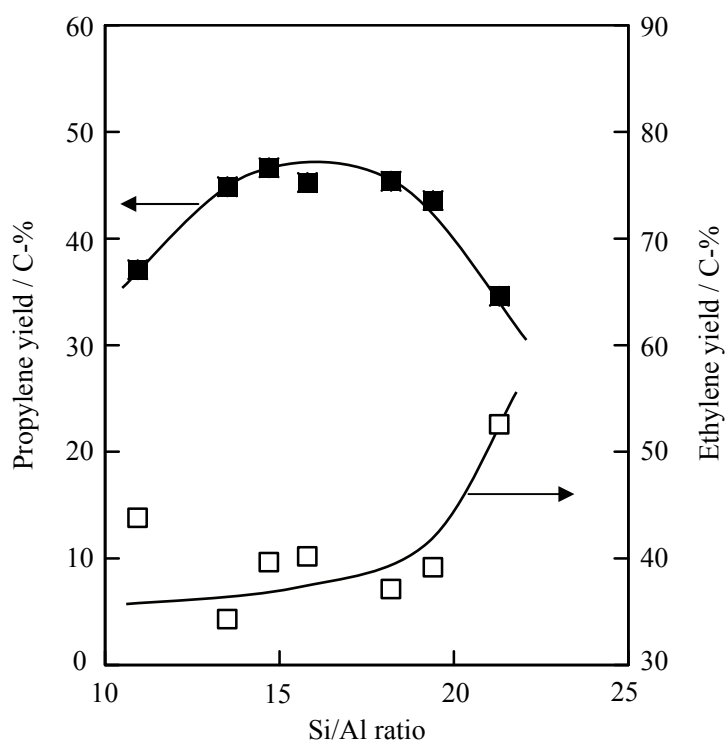
Fig. 7 Relationship between Si/Al ratio of CHA type zeolite and yield of light olefins (($\square$) ethylene and ($\blacksquare$) propylene). Reaction conditions: temp. = 400 °C, W/F = 0.0125 g min mL^{-1}.
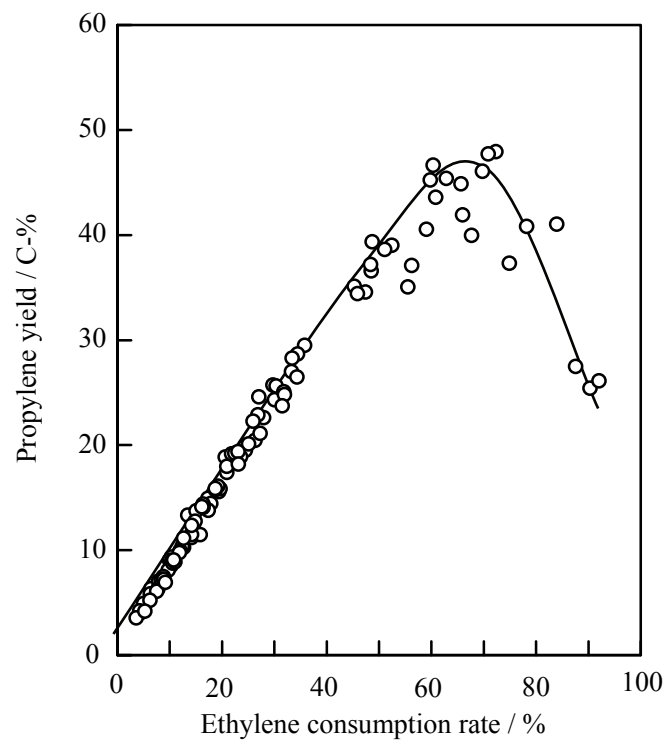
Fig. 8 Propylene yield as a function of ethylene consumption rate for CHA type zeolite obtained with seed crystals.